Contrasting water use characteristics of riparian trees under different water tables along a losing river

Revised manuscript submitted to *Journal of Hydrology* (HYDROL44113)

Yue Li[a, b], Ying Ma[a, b, *], Xianfang Song[a, b, *], Lixin Wang[c], Lihu Yang[a, b], Xiaoyan Li[d,e], Binghua Li[f]

[a] *Key Laboratory of Water Cycle and Related Land Surface Processes, Institute of Geographic Sciences and Natural Resources Research, Chinese Academy of Sciences, Beijing 100101, China*

[b] *University of Chinese Academy of Sciences, Beijing 100049, China*

[c] *Department of Earth Sciences, Indiana University-Purdue University Indianapolis (IUPUI), Indianapolis, IN 46202, United States*

[d] *Beijing Normal University, Faculty Geographical Science, State Key Laboratory Earth Surface Processes & Resource Ecology, Beijing 100875, China*

[e] *Beijing Normal University, School of Nature Resources, Faculty Geographical Science, Beijing 100875, China*

[f] *Beijing Water Science & Technology Institute, Beijing 100048, China*

* *Corresponding author,*

E-mail address: maying@igsnrr.ac.cn (Ying Ma), songxf@igsnrr.ac.cn (Xianfang Song)

This is the author's manuscript of the article published in final edited form as:

Li, Y., Ma, Y., Song, X., Wang, L., Yang, L., Li, X., & Li, B. (2022). Contrasting water use characteristics of riparian trees under different water tables along a losing river. Journal of Hydrology, 611, 128017. https://doi.org/10.1016/j.jhydrol.2022.128017

Abstract

Rivers losing flow into surrounding aquifers ('losing' rivers) are common under changing climates and groundwater overexploitation. The riparian plant-water relations under various water table dynamics along a losing river remain unclear. In this study, the water isotopes (δ^2H and $\delta^{18}O$), leaf $\delta^{13}C$, and MixSIAR model were used combinedly for determining the root water uptake patterns and leaf water use efficiency (WUE) of *Salix babylonica* (L.) at three sites (A, B, and C) with different water table depths (WTDs) in the riparian zone of Jian and Chaobai River in Beijing, China. The correlations of water source contributions with WTD and WUE were quantified. The riparian *S. babylonica* primarily took up upper (0–80 cm) soil water (71.5%) with the lowest leaf $\delta^{13}C$ (−28.8 ± 1.1 ‰) at site A under deep WTD (20.5 ± 0.5 m). In contrast, deep water below 80 cm depth including groundwater contributed 55.1% to *S. babylonica* at site B with fluctuated shallow WTD (1.9 ± 0.4 m), where leaf $\delta^{13}C$ was highest (−27.9 ± 1.0 ‰). The *S. babylonica* mainly used soil water in 30–170 cm layer (56.9%) with mean leaf $\delta^{13}C$ of −28.2 ‰ ± 0.7 ‰ at site C with stable shallow WTD (1.5 ± 0.1 m). It was found that both the contributions of upper soil water in 0–80 cm and deep water below 80 cm had significantly quadratic correlations with WTD under shallow water table conditions ($p < 0.05$). Leaf $\delta^{13}C$ was negatively correlated with contributions of upper soil water above 80 cm depth, but it was positively related to the contributions of deep water below 80 cm in linear functions ($p < 0.001$). The results indicated that 2.1 m was the optimum WTD for riparian trees, because they maximized the use of deep water sources to get the highest WUE. This study provides insights into managing groundwater, surface water resources and riparian afforestation in losing rivers.

Key words: Root water uptake pattern; Water use efficiency; Water table depth; Stable isotopes; Riparian *S. babylonica*; Losing river

1. Introduction

Many rivers are drying up under warming climates and groundwater overexploitation worldwide, which causes serious decline of water table and degradation of riparian vegetation (Rood et al., 2003; Garcia et al., 2017). Ecological water (e.g., excess surface flow or reclaimed water) has been widely used to recharge dry rivers in recent years (Long et al., 2020; He et al., 2021). Widespread loss of riverflow into underlying aquifers occurs where groundwater levels lie below nearby rivers ('losing' rivers) (Winter et al., 1998; Jasechko et al., 2021). The recharge process increases the water availability for riparian vegetation and various species have been planted to restore the riparian ecosystem. However, increased plant transpiration was linked to reduced riverflow and groundwater level (Vanderklein et al., 2014; Missik et al., 2019; Mkunyana et al., 2019), although some studies claimed that transpiration was not closely coupled to riverflow (McDonald et al., 2015). Therefore, investigating the water use characteristics of riparian species is critical to recover the losing rivers especially in water-scarce regions. It will provide critical insights into managing groundwater and surface water resources as well as riparian afforestation under climate change.

The δ^2H and $\delta^{18}O$ have been widely applied to identify the root water uptake patterns of riparian plants (Dawson and Ehleringer, 1991; Wang et al., 2019a; Oerter and Bowen, 2019; Flanagan et al., 2019). Dawson and Ehleringer (1991) utilized deuterium tracer technique to identify that mature trees nearby a perennial stream rarely absorbed the stream water but used

67 water from deeper strata in the Wasatch Mountains of semiarid western USA. However,
68 Oerter and Bowen (2019) revisited the same experimental site in Dawson and Ehleringer
69 (1991) and demonstrated that soil water was the primary source for these streamside trees via
70 the *in situ* soil water vapor isotope measurements. Applying the stable isotope (δ^2H and $\delta^{18}O$)
71 tracer technique, several studies concluded that the distances away from the riverbank as well
72 as seasonal variations of climate could significantly affect water uptake patterns of riparian
73 trees. For example, ripairan trees at distances greater than 5−15 m from the riverbank
74 substantially depended on soil water and groundwater for plant transpiration without water
75 absorpton from the nearby river water throughout the growing season (Mensforth et al., 1994;
76 Qian et al., 2017; Wang et al., 2019a). Shallow soil water recharged by recent precipitation
77 was generally used as the primary water source for riparian plants during wet season, whereas
78 deep soil water and groundwater were principal in dry season (Dawson and Pate, 1996; Wang
79 et al., 2019a). In particular, groundwater is perceived as a reliable and continuous water
80 source for deep-rooted riparian trees indicated by consistent water isotopes of stems and
81 groundwater (Barbeta and Penuelas, 2017; Li et al., 2019).
82 The water table depth (WTD) has great effects on riparian plant water use (Nippert et al.,
83 2010; Chen et al., 2016; Jasechko et al., 2021). Chen et al. (2016) found that desert riparian
84 species under the WTD of 1.8 m used a mixture of soil water below 75 cm depth,
85 groundwater, and river water. Once the WTD increased to 3.8 m and 7.2 m, species mainly
86 relied on deeper soil water below 150 cm and even groundwater. Majority of studies
87 indicated that the increasing WTD induced water uptake pattern adjustments towards deeper
88 water sources (Barbeta et al., 2015; Chen et al., 2016; Li et al., 2019). Nevertheless, some

studies argued that riparian trees switched their water sources from groundwater to vadose-zone soil water in response to the water table decline (Nippert et al., 2010; Busch et al., 1992). Riparian species might change root distributions and develop plastic water uptake patterns in order to acclimate to the variable WTDs (Horton et al., 2001). Therefore, it is necessary to investigate the water uptake patterns for riparian trees under various water table conditions. Furthermore, little is known about the quantitative relationship between the WTD and root water uptake patterns of the riparian plants.

The shift of water sources for riparian plants is mainly driven by leaf transpiration. Leaf water use efficiency (WUE), defining as the ratio of photosynthetic rate and transpiration rate, is a crucial indicator to reflect plant water use characteristics (Farquhar et al., 1989; Wang et al., 2021; Zhao et al., 2021). The plant leaf $\delta^{13}C$ is positively correlated with intrinsic WUE especially for C3 plants and it can be used as an indicator of WUE (Wang et al., 2019b). A growing numbers of evidence showed that plants with higher dependence on deeper water sources were generally linked to higher WUE and survive drought more successfully (Picon-Cochard et al., 2001; Liu et al., 2017; Ding et al., 2020). The WUE of arid and semi-arid deep-rooted plant species was observed to increase with deeper WTD (Si et al., 2015), whereas Antunes et al. (2018) found that there was no response of WUE to increasing WTD for the semi-arid dimorphic-rooted conifer trees. It can be found that most of above studies are located in arid and semi-arid areas. It is still uncertain how WUE of riparian plants coordinates with root water uptake patterns under different WTD conditions in losing rivers.

The aim of this study was to identify and understand water strategies of deep-rooted riparian trees along gradients of WTD, using stable isotopes ($\delta^{2}H$, $\delta^{18}O$ and $\delta^{13}C$) together

111 with the MixSIAR model. Focusing on rivers in Beijing, China, the objectives of this study
112 were (1) to quantify the seasonal water uptake patterns for riparian trees under different
113 WTDs and distances away from the riverbank, (2) to compare the leaf WUE of riparian trees
114 under different WTDs and distances away from the riverbank, (3) to determine the
115 quantitative relationships of water uptake patterns with WTD and leaf WUE. These results
116 will provide insights on riparian ecosystem and water resources management of losing rivers.

117 **2. Materials and methods**

118 *2.1 Study area and field measurements*

119 The experiments of *Salix babylonica* (L.) were conducted from May to November in 2019
120 in the riverside of the Jian and Chaobai River, Beijing, China (40°07′30″N, 116°40′37″E) (Fig.
121 1). A sub-humid monsoon climate with mean temperature of 11.5 ºC and mean relative
122 humidity (RHU) of 60% is dominant in this study area. The multi-year (1961−2021) average
123 precipitation is 532 mm, with 84.5% of which occurring at the rainy season during June 15 and
124 September 15 (Fig. 2). In comparison, the total precipitation in 2019 was 445.6 mm, with
125 73.9% of which concentrated on the rainy season (Fig. 2). Thus, 2019 was identified as a dry
126 year based on the multi-year (1961−2021) rainfall frequency curve. The Jian and Chaobai
127 River were dried up between 1999 and 2007 and have been recharged with ecological water
128 since 2007. *S. babylonica* with deep roots was one of the most widespread planted riparian
129 species in the study area. The maximum rooting depth of *S. babylonica* can reach about 4 m
130 and vary with different water tables (Ferro et al., 2003). Three representative sites (A, B, and C)
131 with different WTDs were selected along the Jian and Chaobai River (Fig. 1). At each site, four
132 plots planted with *S. babylonica* at distance of 5 m, 10 m, 20 m and 45 m away from the

133 riverbank (D05, D10, D20 and D45, respectively) were constructed for field measurements
134 and sample collections (Fig. 1).
135 <Figure 1>
136 A tilting rain gauge of 0.2 mm per tip (SL3-1, Shanghai meteorological instrument,
137 Shanghai, China) was used to record daily precipitation in the meteorological observation
138 station (Fig. 1). The river water level nearby each site was monitored using a doppler open
139 channel flowmeter (HOH-L-01, King Water Co Ltd., Beijing, China). The groundwater level
140 was measured once a month using a pressure-type groundwater stage gauge (HOH-S-Y, King
141 Water Co Ltd., Beijing, China) placed in the monitoring wells. The river water level was
142 observed to fluctuate at 28.4 – 29.4, 27.9 – 28.9, and 26.5 – 27.3 m nearby the sites A, B, and C,
143 respectively (Fig. 2a). The WTD at site A (20.5 m ± 0.5 m) was significantly ($p < 0.01$) deeper
144 than the other two sites B (1.9 m ± 0.4 m) and C (1.5 m ± 0.1 m). The WTD fluctuation was
145 more significant at site B compared with the stable WTD at site C (Fig. 2b).
146 <Figure 2>
147 *2.2 Sample collection*
148 Six field campaigns were conducted to collect water samples of river, groundwater,
149 precipitation, soil, and stem for δ^2H and $\delta^{18}O$ measurements as well as plant leaf samples for
150 $\delta^{13}C$ analysis on May 5, June 14, July 26, August 15, September 26, and November 5. River
151 water nearby each site was sampled by means of a hydrophore, while a sucking pump was
152 used to collect groundwater in monitoring wells. Precipitation was sampled using a device
153 consisted of a polyethylene bottle, a funnel and plastic ball during the observation period
154 (Sun et al., 2019).

One riparian *S. babylonica* (with diameter of 23 ± 3 cm at breast height) in each plot was selected to measure the water stable isotopes in stem and leaf $\delta^{13}C$ (Fig. 1). Several suberized and mature stems were sampled from each *S. babylonica* and removed the phloem and bark to prevent isotopic contamination. Stems were put into 12-ml glass vials and kept refrigerated before stem water extraction and isotope analysis. Mature foliage (approximately 50 leaves) from branches at similar heights (4–5 m) of *S. babylonica* tree was collected for plant leaf $\delta^{13}C$ analysis. The collected leaves were oven-dried at 65 °C for at least 64 h until they reached a constant mass on the day of sampling. Subsequently, leaf samples were ground into fine powder and sieved using a 0.15 mm mesh screen.

Soil cores within 1 m of each *S. babylonica* tree in the four plots were obtained by a power auger (CHPD78, Christie Engineering Company, Sydney, Australia). The soil samples were collected at depths of 0–5, 5–10, 10–15, 15–20, 20–30, 30–40, 40–60, 60–80, 90–110, 150–170, 190–210, 250–270, and 280–300 cm. They were removed roots, put into 12-ml glass vials and kept frozen in a refrigerator before soil water extraction and isotope analysis. Soil was also sampled to measure the gravimetric soil water content (SWC) using the oven-dry method at the same depths listed above.

2.3 Isotopic analyses

Water in stem and soil samples was extracted using the automatic cryogenic vacuum distillation system (LI-2100, LICA, Beijing, China). The whole extraction progress lasted for 3 h and the extraction efficiency was all up to 99% to ensure no isotopic fractionation. The isotopic ratio infrared spectroscopy (IRIS) system (DLT-100, Los Gatos Research, Mountain View, USA) was applied to measure the $\delta^{2}H$ and $\delta^{18}O$ in precipitation, river water, soil water,

and groundwater. To avoid the organic contaminants during IRIS measurements, the isotopic composition of stem water was analyzed using the Isotope Ratio Mass Spectrometry (IRMS) system (MAT253, Thermo Fisher Scientific, Bremen, Germany). The measuring precisions of both IRIS and IRMS system were ±1‰ for δ^2H and ± 0.1‰ for $\delta^{18}O$ in different water samples, respectively. The measured δ^2H and $\delta^{18}O$ were then calibrated with the Vienna Standard Mean Ocean Water (VSMOW) (Sun et al., 2019; Zhao and Wang, 2021). There was no significant difference in δ^2H and $\delta^{18}O$ measurements for soil water, groundwater, precipitation and river water analyzed by the IRMS and IRIS systems (Li et al., 2021). The $\delta^{13}C$ in plant leaf was measured using the IRMS system (MAT253, Thermo Fisher Scientific, Bremen, Germany) with a precision of ± 0.15‰. The measured $\delta^{13}C$ in plant leaf was calibrated with the Vienna Pee Dee Belemnite (V–PDB).

2.4 MixSIAR model

The MixSIAR model v3.1 (Stock and Semmens, 2016) coupled with δ^2H and $\delta^{18}O$ isotopes was applied to identify the potential water source contributions to riparian *S. babylonica*. Because the WTD was much deeper than the maximum rooting depth of *S. babylonica* trees at site A, groundwater could not be taken up by trees. In light of the water isotopic composition and SWC distributions in the profile, soil water in the four layers of 0–30, 30–80, 80–170, and 170–300 cm were classified as the potential water sources of *S. babylonica* trees at site A. Since water isotopic values of groundwater were similar to those of soil water in the 170–300 cm layer, they had been merged into one potential water source (soil water in 170–300 cm layer) besides the soil water sources in the 0–30 cm, 30–80 cm, and 80–170 cm layers for *S. babylonica* trees under shallow WTD sites B (1.9 m ± 0.4 m) and C (1.5 m ± 0.1 m). These

199 isotopic compositions of potential water sources were referred as source data in the MixSIAR
200 model, while the mixture data was set as the δ^2H corrected by potential water source line (PWL)
201 correction method (Li et al., 2021) and raw $\delta^{18}O$ in stem water. More details about the
202 MixSIAR model parameter settings were given in Li et al. (2021).

203 *2.5 Statistical analysis*

204 The seasonal differences in the isotopes of different water bodies, SWC, proportional
205 contributions of water sources, and plant leaf $\delta^{13}C$ values among the three sites as well as those
206 among the four plots at different distances away from the riverbank were evaluated by the
207 One-way analysis of variance (ANOVA) incorporating with post-hoc Tukey's,
208 Kolmogorov-Smirnov and Levene's tests ($p < 0.05$) (Sun et al., 2018). Regression analyses
209 were performed to quantify the relationships of water source contributions with WTD and
210 plant leaf $\delta^{13}C$ values. All statistical analyses were conducted with the SPSS 24.0 software
211 (SPSS Inc., USA).

212 **3. Results**

213 *3.1 Variations of soil water contents and isotopes in different waters*

214 The SWC in different soil layers varied greatly with sampling campaigns and distances
215 away from the riverbank among the sites A, B and C (Fig. 3). The SWC values in upper 0−80
216 cm layer were significantly higher at site A than other two sites throughout the observation
217 period ($p < 0.001$). However, the SWC in 170−300 cm layer at site A was much lower with
218 significantly seasonal variations compared with other two sites ($p < 0.001$). A significant
219 decrease of SWC was observed from May (0.32 g g^{-1}) to July (0.09 g g^{-1}) in 170−300 cm
220 layer at site A. The SWC in 80−170 cm layer was lower but changed greatly with seasons

(standard deviation of 0.8 g g^{-1}) at site B than other two sites. Furthermore, no significant difference in SWC in 0–80 cm layer was found among four distances at site A ($p > 0.05$), but decreasing SWC was found in 170–300 cm layer from D05 to D45 (Fig. S1). The SWC in 80–170 cm layer decreased from D05 to D45 at site B. There was no significant difference in SWC distributions among the four distances at site C ($p = 0.98$) (Fig. S1).

<Figure 3>

<Figure S1>

The isotopes in groundwater at site A (mean of –71.1‰ for δ^2H and –10.2‰ for $\delta^{18}O$) were significantly more depleted than those of groundwater at sites B (mean of –58.9‰ for δ^2H and –7.6‰ for $\delta^{18}O$) and C (mean of –59.4‰ for δ^2H and –7.7‰ for $\delta^{18}O$) ($p < 0.01$) (Fig. 4 and Table S1). There was no significant difference in the isotopic compositions of river water among the three sites ($p > 0.05$). It was obvious that the δ^2H and $\delta^{18}O$ in river water were much more enriched than those in groundwater at all the three sites ($p < 0.05$) (Fig. 4 and Table S1).

The isotopic compositions of soil water had no significant difference in the 0–80 cm layer among the three sites ($p = 0.96$), but they were more enriched below 80 cm at sites B and C compared with those at site A ($p < 0.05$). The slopes of soil water line (SWL) at sites B and C were much lower than those at site A, indicating stronger soil water evaporation at sites B and C. No significant difference in isotopic values of soil water was observed among four plots (D05, D10, D20, D45) at site A ($p = 0.83$). The δ^2H and $\delta^{18}O$ in soil water in the 80–170 cm layer were gradually depleted from D05 to D45 during June and August at site B, while they increased from D05 to D20 but then decreased in plot D45 at site C (Fig. 4 and Table S1). The slope of SWL gradually increased with the increase of distance away from the riverbank at

243 the three sites, suggesting a decrease of soil water evaporation from D05 to D45. The stem
244 water isotopes at sites A and C were slightly depleted than those at site B (Fig. 4 and Table S1).
245 δ^2H and $\delta^{18}O$ in stem water gradually enriched from D05 to D20 at sites A and C, whereas they
246 were depleted from D05 to D45 at site B.
247 <Figure 4>
248 *3.2 Seasonal and spatial variations in root water uptake patterns*
249 The water uptake patterns of riparian *S. babylonica* were strongly different among the
250 three sites (Figs. 5 and 6). *S. babylonica* primarily took up upper soil water in 0−80 cm layer
251 with mean contributions of 71.5% throughout the observation period at site A with deep
252 WTD (Figs. 5a and 6a). The soil water below 80 cm depth primarily contributed to *S.*
253 *babylonica* with proportions more than 55.1% at site B with fluctuated shallow WTD (Figs.
254 5b and 6b). In comparison, the main water source of *S. babylonica* at site C under shallow
255 WTD without significant fluctuation was soil water in 30−170 cm layer with mean
256 contributions of 56.9% throughout the observation period (Figs. 5c and 6c). *S. babylonica* at
257 site A absorbed particularly more soil water in 0−30 cm layer (44.2%) than sites B (20.7%)
258 and C (22.8%) ($p < 0.01$). Moreover, the proportional contributions of soil water in 170-300
259 cm layer or groundwater to *S. babylonica* were significantly different among sites A (13.6%),
260 B (28.3%), and C (18.3%) ($p < 0.01$) (Fig. 6).
261 The contributions of potential water sources to *S. babylonica* exhibited significantly
262 seasonal differences among the three sties ($p < 0.05$). A decrease of the soil water
263 contribution below 80 cm depth associated with an increase in 0−80 cm layer was shown
264 with the growth of *S. babylonica* trees at site A (Fig. 5a). The soil water contribution in

80–170 cm layer to *S. babylonica* decreased significantly (21.6%) during June to August with a water table decline (0.8 m) at site B (Fig. 5b) ($p < 0.05$). Meanwhile, *S. babylonica* water uptake from surficial soil water in 0–30 cm layer increased by 20.0% during rainy season ($p < 0.05$). *S. babylonica* trees at site C kept reducing the water uptake proportions in 30–80 cm layer from May (46.7%) to November (17.7%), while groundwater contributions increased by 10.7% (Fig. 5c) ($p < 0.05$). Although significant seasonal differences in riparian tree water uptake depths were observed ($p < 0.05$), there was no general and significant correlation between environmental factors (e.g., air temperature, RHU, and precipitation) and upper soil water (0–80 cm) contribution to riparian trees at the three sites ($p > 0.05$) (Fig. S2).

The water use characteristics of *S. babylonica* varied distinctly along the distance away from the riverbank at the three sites. The superficial (0–30 cm) soil water contributions increased significantly by 23.0% from D05 to D20 ($p < 0.05$), whereas deep (170–300 cm) soil water contributions to *S. babylonica* reduced by 6.4% from D05 to D45 at site A (Fig. 6a). The *S. babylonica* took up more groundwater but less soil water in 80–170 cm layer from D05 to D45 at site B (Fig. 6b). In particular, the groundwater contribution to *S. babylonica* at D20 and D45 significantly increased by an average of 14.4% when the water table declined from 1.7 m to 2.5 m at site B ($p < 0.05$). On the contrary, *S. babylonica* reduced water absorption (47.3%) from deep water below 80 cm but accessed more upper soil water (28.6%) significantly ($p < 0.05$) in response to the 0.8 m decline of WTD at D05 and D10 at site B ($p < 0.05$). At site C, the contributions of deep water below 80 cm depth reduced remarkably (20.2%) from D05 to D45, whereas the upper soil water increased the contributions (14.1%) to *S. babylonica* from D05 to D20 (Fig. 6c) ($p < 0.05$).

<Figure 5>

<Figure 6>

3.3 Changes in leaf $\delta^{13}C$ of riparian trees

The leaf $\delta^{13}C$ values at the three sites varied differently with increasing distance from the riverbank during the observation period (Fig. 7). Riparian trees at site A had significantly lower leaf $\delta^{13}C$ values (mean of −28.8‰) than those at the other two sites B (mean of −27.9‰) and C (mean of −28.1‰) ($p < 0.05$). There was a significant decrease of leaf $\delta^{13}C$ value (2.3‰) from D05 to D20 at site A ($p < 0.05$). However, the $\delta^{13}C$ values generally increased with increasing distance from the riverbank (ranging from −28.8‰ at D05 to −27.0‰ at D45) at site B. It was found that the leaves of *S. babylonica* at D20 and D45 had significantly higher $\delta^{13}C$ values (mean of −27.1‰) than those at other two distances (mean of −28.7‰) at site B ($p < 0.05$). The leaf $\delta^{13}C$ of the *S. babylonica* nearest the riverbank (mean of −27.6‰ at D05) at site C was higher than that at other distances (mean of −28.4‰) (Fig. 7). Significant seasonal differences in the leaf $\delta^{13}C$ values were shown among the three sites ($p < 0.05$) (Table S2). The $\delta^{13}C$ values in the tree leaves were the lowest in May (mean of −28.7‰) and August (mean of −28.7‰). The leaf $\delta^{13}C$ in plot D05 at site C showed an increasing trend with the growth of *S. babylonica* compared with that at sites A and B (Table S2). Nevertheless, no significant regression relationship between leaf $\delta^{13}C$ value of *S. babylonica* and environment factors (e.g., air temperature, RHU, and precipitation) was observed at the tree sites ($p > 0.05$) (Fig. S3).

<Figure 7>

4. Discussion

4.1 Impacts of water table depth on riparian tree water uptake pattern

This study indicated that the depth and fluctuation of water table diversified the water uptake patterns of riparian trees near the losing river (Naumburg et al., 2005; Simunek and Hopmans, 2009; Fan et al., 2017; Antunes et al., 2018). It agreed well with previous studies that riparian trees primarily took up soil water in upper 0−80 cm layer under deep WTD with weaker hydraulic connections between the river and underlying groundwater system (Figs. 5a and 6a) (Wu et al., 2021). An evident shift of the main water uptake depth of riparian trees from soil water in 30−80 cm layer towards deeper soil layers or groundwater was found when the WTD increased from 1.5 ± 0.1 m to 1.9 ± 0.4 m under shallow WTD condition with closer river water-groundwater interactions in this study (Figs. 5b, 5c, 6b and 6c). It suggested that the deep-root growth and their water uptake capabilities were limited under shallow WTD without significant fluctuations (1.5 ± 0.1 m) (Figs. 5c and 6c) or oxygen stress conditions (Naumburg et al., 2005; Fan et al., 2017). Nevertheless, riparian trees could gradually acclimate to persistently shallow WTD environment with plant growth indicated by an increase of groundwater utilization (10.7%) for riparian trees from May to November (Figs. 5c and 6c) (Naumburg et al., 2005). In addition, these riparian trees closer to the stream generally had better ability to adapt to oxygen stress, which could be derived from the decreasing deep-water contributions along the distance away from riverbank (Fig. 6c). Fluctuated shallow WTD could motivate riparian trees to develop a dimorphic-root system and switch their water main uptake depths between the shallow soil layers and deep layers (Figs. 5b and 6b) (Zencich et al., 2002). But the responses to water table decline of riparian

330 trees at different distances at fluctuated WTD area differed significantly with reducing water
331 absorption from deep water below 80 cm at distance within 10 m and increasing groundwater
332 utilization at distance of 20 m and 45 m away from the riverbank (Figs. 5b and 6b). The
333 stimulation of deep-roots helped riparian trees susceptible to drought stress at distance greater
334 than 20 m from the riverbank survive from the climate drought (Ehleringer and Dawson,
335 1992; Antunes et al., 2018; Li et al., 2019) or river water level lowering during rainy season
336 as shown in this study (Figs. 3c and 5b).

337 The quantitative relationship between the shallow WTD and contributions of different
338 water sources to riparian trees was not discovered in previous studies. In our study, a
339 significantly quadratic relationship was found between the WTD and proportional
340 contributions of upper soil water in 0−80 cm layer ($R^2 = 0.43$, $p < 0.05$) at shallow WTD
341 areas (Sites B and C) (Fig. 8a). Meanwhile, the WTD had a significant quadratic correlation
342 with deep-water contributions below 80 cm depth ($R^2 = 0.43$, $p < 0.05$) (Fig. 8b). Particularly,
343 riparian *S. babylonica* at constant shallow WTD sites (WTD < 1.7 m) increased deep water
344 absorption with increasing WTD, whereas those under fluctuated shallow WTD (1.7−2.5 m)
345 showed an increase and then decrease of deep-water contribution as water table declined (Fig.
346 8b). The upper soil water contribution was minimum at the WTD of 2.1 m, when the
347 deep-water contribution reached a maximum value. It could be explained that declining water
348 tables (WTD increased from 1.5 m to 2.1 m) aerated deep soil layers, benefited for new
349 deep-root exploitation and further stimulated riparian trees to utilize deep water when
350 groundwater severely restricted the active root zone of riparian trees under oxygen stress
351 (Naumburg et al., 2005). However, riparian trees can tolerate declining water table only up to

352 a species-specific threshold value, beyond which drought stress occurred (Sperry et al., 1998).
353 In this study, when the WTD exceeded 2.1 m, deeper water tables could reduce the
354 availability of a permanent water source for riparian trees and therefore lead to water stress
355 (Naumburg et al., 2005; Wang et al., 2019a). Therefore, water stress and oxygen stress
356 resulting from fluctuated WTD had a great effect on riparian tree water uptake patterns.
357 Specifically, higher water tables without evident fluctuations generally killed flooded roots
358 because most species cannot tolerate the associated low oxygen levels (Naumburg et al., 2005;
359 Li et al., 2019). The appropriately decreasing water tables benefited plant species from
360 avoiding oxygen stress, but the excessive water table decline probably resulted in plant water
361 stress (Naumburg et al., 2005; Li et al., 2019). Our findings suggested that 2.1 m was the
362 optimum WTD to utilize the deep water sources for the riparian trees development in the face
363 of drought and oxygen scarce environment.
364 <Figure 8>
365 *4.2 Relationship between riparian tree water uptake depth and water use efficiency*
366 It was evident that there were tradeoff and coordination between plant water uptake depth
367 and WUE near rivers, because significant difference of WUE was observed in riparian trees
368 among the four plots at different distances from the riverbank at three sites with various root
369 water uptake patterns (Figs. 5, 6 and 7). Plants with shallow root water uptake depths (such as
370 *S. babylonica* at deep WTD at site A) mainly relied on upper soil water which was subjected
371 to fast evaporation loss (Figs. 5a and 6a). They generally had rapid water resource capture
372 and large transpiration rates (Ding et al., 2020; Nie et al., 2019; Antunes et al., 2018), leading
373 to lower leaf $\delta^{13}C$ and WUE values (Figs. 5a and 7). Moreover, the increase in shallow soil

374 water contributions was linked to the obviously decreasing leaf $\delta^{13}C$ and WUE values as the
375 distance from the riverbank increased (from 5 m to 20 m) at deep WTD site (Figs. 5a and 7).
376 When the riparian trees primarily depended on deep water sources in fluctuated shallow
377 WTD area (such as *S. babylonica* at site B), leaf $\delta^{13}C$ and WUE increased significantly
378 particularly at the lowering of the water table (Figs. 5b and 7). The increasing deep water
379 contributions accompanied with growing leaf $\delta^{13}C$ and WUE were further found along the
380 distance away from riverbank at high water table site with evident fluctuations. This could be
381 likely due to that stomatal conductance and transpiration rate reduced with the decreasing
382 deep soil moisture to avoid hydraulic failure and drought stress (Klein et al., 2013;
383 Martinez-Vilalta and Garcia-Forner, 2017; Ding et al., 2020). Pezeshki et al. (1998) and Li et
384 al. (2006) also indicated that the anoxia could reduce the plant stomatal conductance and
385 transpiration rate. Our findings confirmed that deep-root water uptake and leaf transpiration
386 rate of riparian trees in anaerobiosis environment were restricted under the constant shallow
387 WTD condition (Figs. 5c and 7).

388 The relationship between the riparian tree water uptake depth and WUE was not
389 quantified in previous studies. As shown in Fig. 9a, this study clarified that the leaf $\delta^{13}C$ was
390 significantly negatively correlated with the contributions of upper soil water in 0−80 cm layer
391 ($R^2 = 0.47$, $p < 0.001$). Meanwhile, significantly positive relationships were found between
392 leaf $\delta^{13}C$ and contributions of deep water below 80 cm depth ($R^2 = 0.42$, $p < 0.001$) (Fig. 9b).
393 These linear relationships indicated that increasing reliance on upper soil water sources
394 linearly declined the leaf $\delta^{13}C$ and WUE of riparian trees (Fig. 9a), while the growing
395 dependence on deeper water sources proportionally increased the WUE of riparian trees (Fig.

396 9b). Riparian trees mainly relied on upper soil water sources fed by recent precipitation in
397 wet season (Dawson and Pate, 1996; Wang et al., 2019a). The easier soil water accessibility
398 stimulated riparian trees to maximize their growth and transpiration during the rainy season,
399 which resulted in the lower WUE and water use without water limitation (Cao et al., 2020;
400 Wu et al., 2021). Deep water was critical for plant water use and growth especially under
401 drought stress (Cao et al., 2020). However, the main root water uptake depth shift from
402 shallow layers towards deep layers (i.e., increasing reliance on deeper water sources)
403 generally caused riparian trees to consume more energy due to new deep-root growth, longer
404 water transport path and greater water transport resistance of deep-roots (Cao et al., 2020).
405 Therefore, riparian trees used deeper water effectively and conservatively through stomatal
406 closure and the lowering of transpiration rate, leading to higher leaf $\delta^{13}C$ and WUE values. It
407 agreed well with previous studies that the root water uptake depth adjustments towards
408 deeper layers during dry season could cause a 13% reduction of the total annual transpiration
409 and a 15% increase of the WUE of evergreen *Ligustrum lucidum* (Wu et al., 2021).
410 <Figure 9>
411 *4.3 Implications and further scopes of this study*
412 This study indicated that riparian deep-rooted trees were strongly dependent on shallow
413 soil water recharged by precipitation and remained high transpiration rates (low WUE) under
414 deep WTD. The continuously large plant water consumption could result in a dried upper soil
415 layer especially during drought season, increasing the risk of canopy defoliation, mortality
416 and degradation of riparian trees (Nie et al., 2014; Wang and D'Odorico, 2019; Ding et al.,
417 2020). Large-scale afforestation will not be recommended in this area, while shallow-rooted

418 herbs with less vulnerable to drought and lower water demand for transpiration may be
419 suitable for vegetation restoration in the riparian zone. A shift of shallow and deep-root water
420 uptake depths with higher WUE could help riparian trees acclimate to decreasing deep water
421 accessibilities under fluctuated shallow WTD (Dawson and Pate, 1996; Wang et al., 2019a).
422 Moreover, the higher WUE of riparian trees was generally linked to reducing water
423 consumption for transpiration without affecting plant growth and maintaining/reserving
424 riverflow and groundwater level, which benefited for balancing the growth of riparian trees and
425 bank storage to avoid loss of riverflow (Vanderklein et al., 2014; Barbeta et al., 2015; Missik et
426 al., 2019; Mkunyana et al., 2019). When the water table continously declined and WTD
427 exceeded 2.1 m, deep water contributions to riparian trees as well as WUE decreased,
428 indicating that the ability to cope with drought stress decreased. In comparison, deep-root
429 development of trees was inhibited and photosynthetic/transpiration decreased due to
430 anaerobiosis when the water table kept high without evident fluctuation. Therefore, the
431 optimum WTD of 2.1 m for best growth of riparian trees was recommended under shallow
432 WTD condition. The sustainability of riparian afforestation must consider both root water
433 uptake depths and plant physiological traits.
434 This study provides a critical insight into evaluating the riparian plant-water relations
435 along a losing river. However, several issues still require further investigations. Firstly, the
436 stable isotopes should be combined with measurements of root distribution and transpiration
437 rate under more water table conditions in different represent years (i.e., dry, normal and wet
438 year) to further analyze the plant-water relationships. Secondly, whether there is a water use
439 competition between trees, shrubs and herbs in the riparian zone is unclear. It is valuable to

compare the water use characteristics among various riparian species in response to different losing river water-groundwater interactions. Thirdly, numerical simulation model can be combined with stable isotopes to trace the transport of water isotopes in groundwater-soil-plant-atmosphere continuum and determine the dynamic characteristics of plant water use (Simunek and Hopmans, 2009; Zhou et al., 2021).

5. Conclusions

In this study, the water use characteristics of deep-rooted *S. babylonica* in the riparian zone under various WTDs along a losing river were determined by the stable isotopes (δ^2H and $\delta^{18}O$ in water as well as leaf $\delta^{13}C$) and MixSIAR model. Our results indicated that the seasonal water uptake patterns and WUE of riparian *S. babylonica* were significantly affected by WTD. Riparian trees accessed more upper soil water and had lower leaf $\delta^{13}C$ under deep WTD (about 20 m) compared to those under shallow WTD (< 2.5 m). A shift of shallow and deep root water uptake depths with higher WUE helped riparian trees adapt decreasing deep water accessibilities under fluctuated shallow WTD (1.9 ± 0.4 m). Nevertheless, deep-root water uptake capabilities and transpiration rate were limited when the water table kept high without evident fluctuation (1.5 ± 0.1 m). Both the water source contributions in upper layer (0−80 cm) and deep layer (below 80 cm depth) were parabolic functions of WTD ($p < 0.05$) when groundwater was shallow. Leaf $\delta^{13}C$ had a positive linear correlation with proportional contribution of deep water ($p < 0.001$). It seemed that 2.1 m was the optimum WTD for riparian trees under shallow WTD, since they could make best use of deep-water sources and remained the highest WUE under water deficit. The higher WUE of riparian trees was advantageous for balancing plant water use and bank storage to avoid large loss of river flow.

However, large-scale afforestation will not be recommended in the area with deep WTD, which may result in a dried upper soil layer especially during drought season and increase the risk of degradation of riparian trees. The sustainability of riparian vegetation restoration should consider both the development of root water uptake depths and physiological traits of plants under different water table conditions.

Acknowledgements

This work was supported by the National Natural Science Foundation of China (41730749, 41671027). LW acknowledges partial support from the Division of Earth Sciences of National Science Foundation (EAR-1554894). Sincere thanks go to Xue Zhang and Yiran Li for their assistance in experiments. We thank the associate editor and the two anonymous reviewers for their professional comments which help us greatly improve the overall quality of the manuscript.

References

Antunes, C., Barradas, M.C.D., Vieira, S., Zunzunegui, M., Pereira, A., Anjos, A., Correia, O., Pereira, M.J., Maguas, C., 2018. Contrasting plant water-use responses to groundwater depth in coastal dune ecosystems. Functional Ecology. 32, 1931-1943.

Barbeta, A., Mejia-Chang, M., Ogaya, R., Voltas, J., Dawson, T.E., Penuelas, J., 2015. The combined effects of a long-term experimental drought and an extreme drought on the use of plant-water sources in a Mediterranean forest. Global Change Biology. 21, 1213-1225.

Barbeta, A., Penuelas, J., 2017. Relative contribution of groundwater to plant transpiration

484 estimated with stable isotopes. Scientific Reports. 7, 1-10.
485 https://doi.org/10.1038/s41598-017-09643-x.
486 Busch, D.E., Ingraham, N.L., Smith, S.D., 1992. Water-uptake in woody riparian
487 phreatophytes of the Southwestern United States: A stable isotope study. Ecological
488 Applications. 2, 450-459.
489 Cao, M., Wu, C., Liu, J., Jiang, Y., 2020. Increasing leaf $\delta^{13}C$ values of woody plants in
490 response to water stress induced by tunnel excavation in a karst trough valley: Implication
491 for improving water-use efficiency. Journal of Hydrology. 586, 124895.
492 https://doi.org/10.1016/j.jhydrol.2020.124895.
493 Chen, Y.P., Chen, Y.N., Xu, C.C., Li, W.H., 2016. The effects of groundwater depth on water
494 uptake of *Populus euphratica* and *Tamarix ramosissima* in the hyperarid region of
495 Northwestern China. Environmental Science and Pollution Research. 23, 17404-17412.
496 Dawson, T.E., Ehleringer, J.R., 1991. Streamside trees that do not use stream water. Nature.
497 350, 335-337.
498 Dawson, T.E., Pate, J.S., 1996. Seasonal water uptake and movement in root systems of
499 Australian phraeatophytic plants of dimorphic root morphology: A stable isotope
500 investigation. Oecologia. 107, 13-20.
501 Ding, Y.L., Nie, Y.P., Chen, H.S., Wang, K.L., Querejeta, J. I., 2020. Water uptake depth is
502 coordinated with leaf water potential, water‐use efficiency and drought vulnerability in
503 karst vegetation. New Phytologist. 229, 1-15.
504 Ehleringer, J.R., Dawson, T.E., 1992. Water-uptake by plants-perspectives from stable isotope
505 composition. Plant Cell and Environment. 15, 1073-1082.

506 Fan, Y., Miguez-Macho, G., Jobbagy, E.G., Jackson, R.B., Otero-Casal, C., 2017. Hydrologic
507 regulation of plant rooting depth. Proceedings of the National Academy of Sciences of the
508 United States of America. 114, 10572-10577.
509 Farquhar, G.D., Ehleringer, J.R., Hubick, K.T., 1989. Carbon isotope discrimination and
510 photosynthesis. Annual Review of Plant Physiology and Plant Molecular Biology. 40,
511 503-537.
512 Ferro, A., Gefell, M., Kjelgren, R., Lipson, D.S., Zollinger, N., Jackson, S., 2003.
513 Maintaining hydraulic control using deep rooted tree systems. In: Tsao, D. (Eds).
514 Advances in Biochemical Engineering-Biotechnology. Springer-Verlag., Berlin, pp.
515 125-156.
516 Flanagan, L.B., Orchard, T.E., Tremel, T.N., Rood, S.B., 2019. Using stable isotopes to
517 quantify water sources for trees and shrubs in a riparian cottonwood ecosystem in flood
518 and drought years. Hydrological Processes. 33, 3070-3083.
519 Garcia, C., Amengual, A., Homar, V., Zamora, A., 2017. Losing water in temporary streams
520 on a Mediterranean island: Effects of climate and land-cover changes. Global and
521 Planetary Change. 148, 139-152.
522 He, Z. K., Han, D.M., Song, X.F., Yang, L.H., Zhang, Y.H., Ma, Y., Bu, H.M., Li, B.H., Yang,
523 S.T., 2021. Variations of groundwater gynamics in alluvial aquifers with reclaimed water
524 restoring the overlying river, Beijing, China. Water. 13, 806.
525 https://doi.org/10.3390/w13060806.
526 Horton, J.L., Kolb, T.E., Hart, S.C., 2001. Responses of riparian trees to interannual variation
527 in ground water depth in a semi-arid river basin. Plant Cell and Environment. 24,

293-304.

Jasechko, S., Seybold, H., Perrone, D., Fan, Y., Kirchner, J.W., 2021. Widespread potential loss of streamflow into underlying aquifers across the USA. Nature. 591, 391-395.

Klein, T., Shpringer, I., Fikler, B., Elbaz, G., Cohen, S., Yakir, D., 2013. Relationships between stomatal regulation, water-use, and water-use efficiency of two coexisting key Mediterranean tree species. Forest Ecology and Management. 302, 34-42.

Li, E.G., Tong, Y.Q., Huang, Y.M., Li, X.Y., Wang, P., Chen, H.Y., Yang, C.Y., 2019. Responses of two desert riparian species to fluctuating groundwater depths in hyperarid areas of Northwest China. Ecohydrology. 12, e2078. https://doi.org/10.1002/eco.2078.

Li, S.W., Pezeshki, S.R., Shields, F.D., 2006. Partial flooding enhances aeration in adventitious roots of black willow (*Salix nigra*) cuttings. Journal of Plant Physiology. 163, 619-628.

Li, Y., Ma, Y., Song, X.F., Wang, L.X., Han, D.M., 2021. A δ^2H offset correction method for quantifying root water uptake of riparian trees. Journal of Hydrology. 593, 125811. https://doi.org/10.1016/j.jhydrol.2020.125811.

Liu, B., Guan, H.D., Zhao, W.Z., Yang, Y.T., Li, S.B., 2017. Groundwater facilitated water-use efficiency along a gradient of groundwater depth in arid northwestern China. Agricultural and Forest Meteorology. 233, 235-241.

Long, D., Yang, W.T., Scanlon, B.R., Zhao, J.S., Liu, D.G., Burek, P., Pan, Y., You, L.Z., Wada, Y., 2020. South-to-North Water Diversion stabilizing Beijing's groundwater levels. Nature Communications. 11, 3665. https://doi.org/10.1038/s41467-020-17428-6.

Martinez-Vilalta, J., Garcia-Forner, N., 2017. Water potential regulation, stomatal behaviour

and hydraulic transport under drought: deconstructing the iso/anisohydric concept. Plant Cell and Environment. 40, 962-976.

McDonald, A.K., Wilcox, B.P., Moore, G.W., Hart, C.R., Sheng, Z.P., Owens, M.K., 2015. Tamarix transpiration along a semiarid river has negligible impact on water resources. Water Resources Research. 51, 5117-5127.

Mensforth, L.J., Thorburn, P.J., Tyerman, S.D., Walker, G.P., 1994. Sources of water used by riparian *Eucalyptus camaldulensis* overlying highly saline groundwater. Oecologia. 100, 21-28.

Missik, J.E.C., Liu, H.P., Gao, Z.M., Huang, M.Y., Chen, X.Y., Arntzen, E., McFarland, D.P., Ren, H.Y., Titzler, P.S., Thomle, J.N., Goldman, A., 2019. Groundwater-river water exchange enhances growing season evapotranspiration and carbon uptake in a semiarid riparian ecosystem. Journal of Geophysical Research-Biogeosciences. 124, 99-114.

Mkunyana, Y.P., Mazvimavi, D., Dzikiti, S., Ntshidi, Z., 2019. A comparative assessment of water use by *Acacia longifolia* invasions occurring on hillslopes and riparian zones in the Cape Agulhas region of South Africa. Physics and Chemistry of the Earth. 112, 255-264.

Naumburg, E., Mata-Gonzalez, R., Hunter, R.G., McLendon, T., Martin, D.W., 2005. Phreatophytic vegetation and groundwater fluctuations: A review of current research and application of ecosystem response modeling with an emphasis on Great Basin vegetation. Environmental Management. 35, 726-740.

Nie, Y.P., Chen, H.S., Ding, Y.L., Zou, Q.Y., Ma, X.Y., Wang, K.L., 2019. Qualitative identification of hydrologically different water sources used by plants in rock-dominated environments. Journal of Hydrology. 573, 386-394.

572 Nie, Y.P., Chen, H.S., Wang, K.L., Ding, Y.L., 2014. Seasonal variations in leaf $\delta^{13}C$ values:
573 implications for different water-use strategies among species growing on continuous
574 dolomite outcrops in subtropical China. Acta Physiologiae Plantarum. 36, 2571-2579.
575 Nippert, J.B., Butler, J.J., Kluitenberg, G.J., Whittemore, D.O., Arnold, D., Spal, S.E., Ward,
576 J.K., 2010. Patterns of Tamarix water use during a record drought. Oecologia. 162,
577 283-292.
578 Oerter, E.J., Bowen, G.J., 2019. Spatio-temporal heterogeneity in soil water stable isotopic
579 composition and its ecohydrologic implications in semiarid ecosystems. Hydrological
580 Processes. 33, 1724-1738.
581 Pezeshki, S.R., Anderson, P.H., Shields, F.D., 1998. Effects of soil moisture regimes on
582 growth and survival of black willow (*Salix nigra*) posts (cuttings). Wetlands. 18, 460-470.
583 Picon-Cochard, C., Nsourou-Obame, A., Collet, C., Guehl, J.M., Eerhi, A., 2001.
584 Competition for water between walnut seedlings (*Juglans regia*) and rye grass (*Lolium*
585 *perenne*) assessed by carbon isotope discrimination and delta O-18 enrichment. Tree
586 Physiology. 21, 183-191.
587 Qian, J., Zheng, H., Wang, P.F., Liao, X.L., Wang, C., Hou, J., Ao, Y.H., Shen, M.M., Liu, J.J.,
588 Li, K., 2017. Assessing the ecohydrological separation hypothesis and seasonal variations
589 in water use by *Ginkgo biloba* L. in a subtropical riparian area. Journal of Hydrology. 553,
590 486-500.
591 Rood, S.B., Braatne, J.H., Hughes, F.M.R., 2003. Ecophysiology of riparian cottonwoods:
592 stream flow dependency, water relations and restoration. Tree Physiology. 23, 1113-1124.
593 Si, J.H., Feng, Q., Yu, T.F., Zhao, C.Y., Li, W., 2015. Variation in Populus euphratica foliar

carbon isotope composition and osmotic solute for different groundwater depths in an arid region of China. Environmental Monitoring and Assessment. 187, 705. https://doi.org/10.1007/s10661-015-4890-y.

Simunek, J., Hopmans, J.W., 2009. Modeling compensated root water and nutrient uptake. Ecological Modelling. 220, 505-521.

Stock, B.C. and Semmens, B.X., 2016. MixSIAR GUI User Manual. Version 3.1. https://github.com/brianstock/MixSIAR/. doi:10.5281/zenodo.47719.

Sun, L., Yang, L., Chen, L.D., Zhao, F.K., Li, S.J., 2018. Hydraulic redistribution and its contribution to water retention during short-term drought in the summer rainy season in a humid area. Journal of Hydrology. 566, 377-385.

Sun, L., Yen, H., Chen, L., Zhao, F.K., Yan, L., 2019. Distribution of agricultural land regulates stream water isotopes over multiple spatial scale in a subtropical forested watershed. Journal of Hydrology. 579. https://doi.org/10.1016/j.jhydrol.2019.124206.

Vanderklein, D.W., Galster, J., Scherr, R., 2014. The impact of Japanese knotweed on stream baseflow. Ecohydrology. 7, 881-886.

Wang, J., Fu, B.J., Jiao, L., Lu, N., Li, J.Y., Chen, W.L., Wang, L.X., 2021. Age-related water use characteristics of Robinia pseudoacacia on the Loess Plateau. Agricultural and Forest Meteorology. 301-302, 108344.

Wang, J., Fu, B.J., Lu, N., Wang, S., Zhang, L., 2019b. Water use characteristics of native and exotic shrub species in the semi-arid Loess Plateau using an isotope technique. Agriculture, Ecosystems and Environment. 276, 55-63.

Wang, L.X., D'Odorico, P., 2019. Water limitations to large-scale desert agroforestry projects

for carbon sequestration. Proceedings of the National Academy of Sciences of the United States of America. 116, 24925-24926.

Wang, P.Y., Liu, W.J., Zhang, J.L., Yang, B., Singh, A.K., Wu, J.E., Jiang, X.J., 2019a. Seasonal and spatial variations of water use among riparian vegetation in tropical monsoon region of SW China. Ecohydrology. 12, e2085. https://doi.org/10.1002/eco.2085.

Winter, T.C., Harvey, J.W., Franke, O.L., Alley, W.M., 1998. Ground water and surface water a single resource. U.S. Geological Survey Circular 1139. U.S. Government Printing Office, Denver, Colorado.

Wu, Z., Behzad, H.M., He, Q.F., Wu, C., Bai, Y., Jiang, Y.J., 2021. Seasonal transpiration dynamics of evergreen Ligustrum lucidum linked with water source and water-use strategy in a limestone karst area, southwest China. Journal of Hydrology. 597, 126199. https://doi.org/10.1016/j.jhydrol.2021.126199.

Zencich, S.J., Froend, R.H., Turner, J.V., Gailitis, V., 2002. Influence of groundwater depth on the seasonal sources of water accessed by *Banksia* tree species on a shallow, sandy coastal aquifer. Oecologia. 131, 8-19.

Zhao, Y., Wang, L., 2021. Insights into the isotopic mismatch between bulk soil water and *Salix matsudana* Koidz trunk water from root water stable isotope measurements. Hydrology and Earth System Sciences. 25, 3975-3989.

Zhao, Y., Wang, L., Knighton, J., Evaristo, J., Wassen, M., 2021. Contrasting adaptive strategies by Caragana korshinskii and Salix psammophila in a semiarid revegetated ecosystem. Agricultural and Forest Meteorology. 300, 108323.

https://doi.org/10.1016/j.agrformet.2021.108323.

Zhou, T.T., Simunek, J., Braud, I., 2021. Adapting HYDRUS-1D to simulate the transport of soil water isotopes with evaporation fractionation. Environmental Modelling & Software. 143, 1-18. https://doi.org/10.1016/j.envsoft.2021.105118.

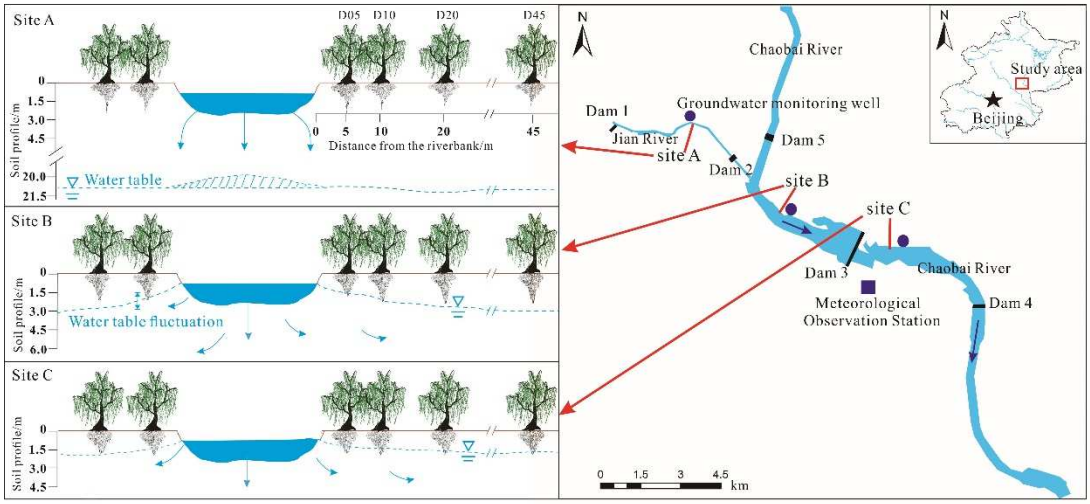

Fig. 1. Location of the study area and three representative sampling sites (A, B, and C). D05, D10, D20, and D45 at each site are the plots at distance of 5 m, 10 m, 20 m, and 45 m away from the riverbank, respectively.

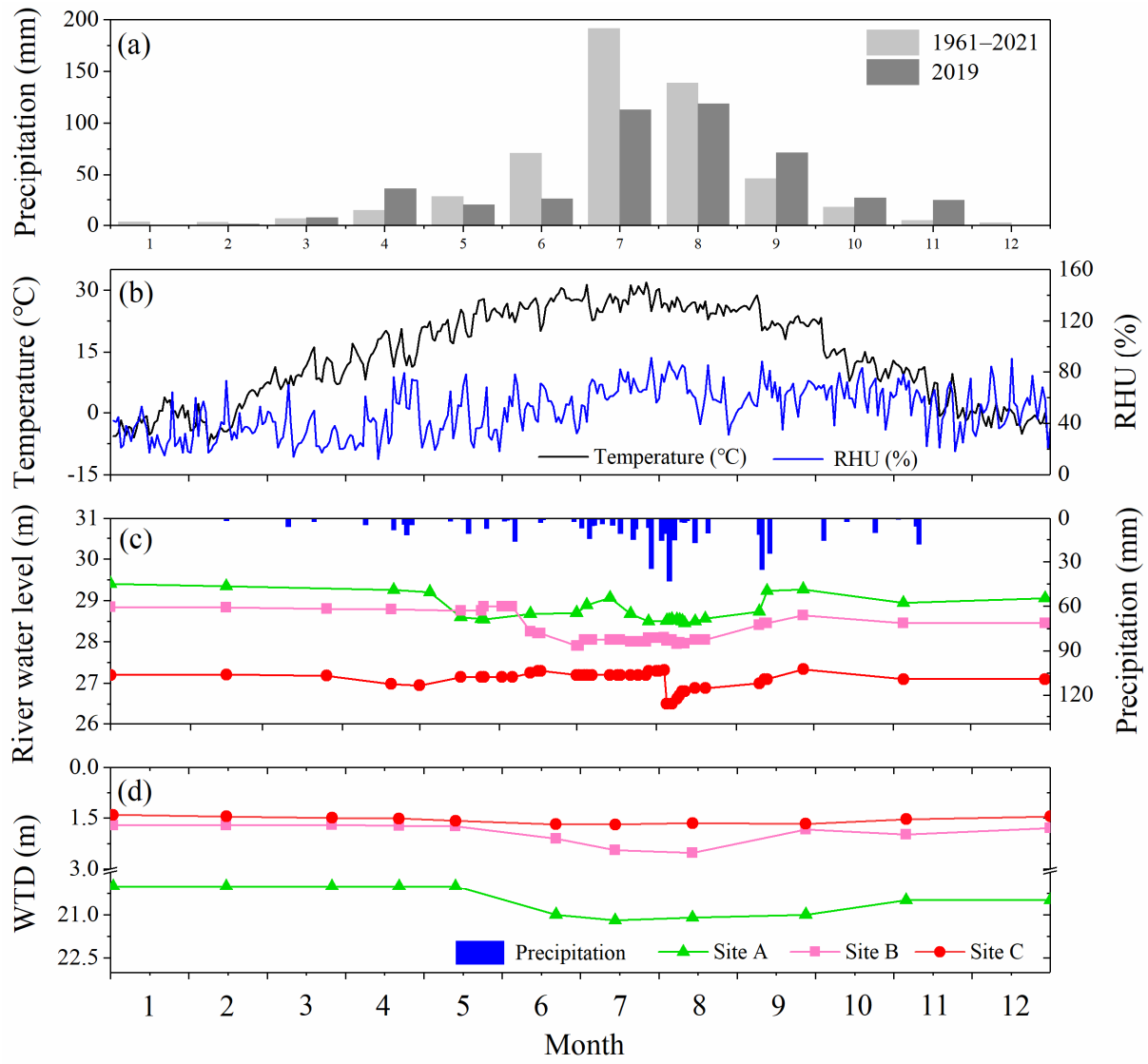

Fig. 2. (a) Monthly average precipitation for multi-year (1961–2021) and the observation period (2019), diurnal variation in (b) temperature and relative humidity (RHU), and seasonal changes in (c) river water level and precipitation, and (d) water table depth (WTD) at sites A, B, and C in 2019.

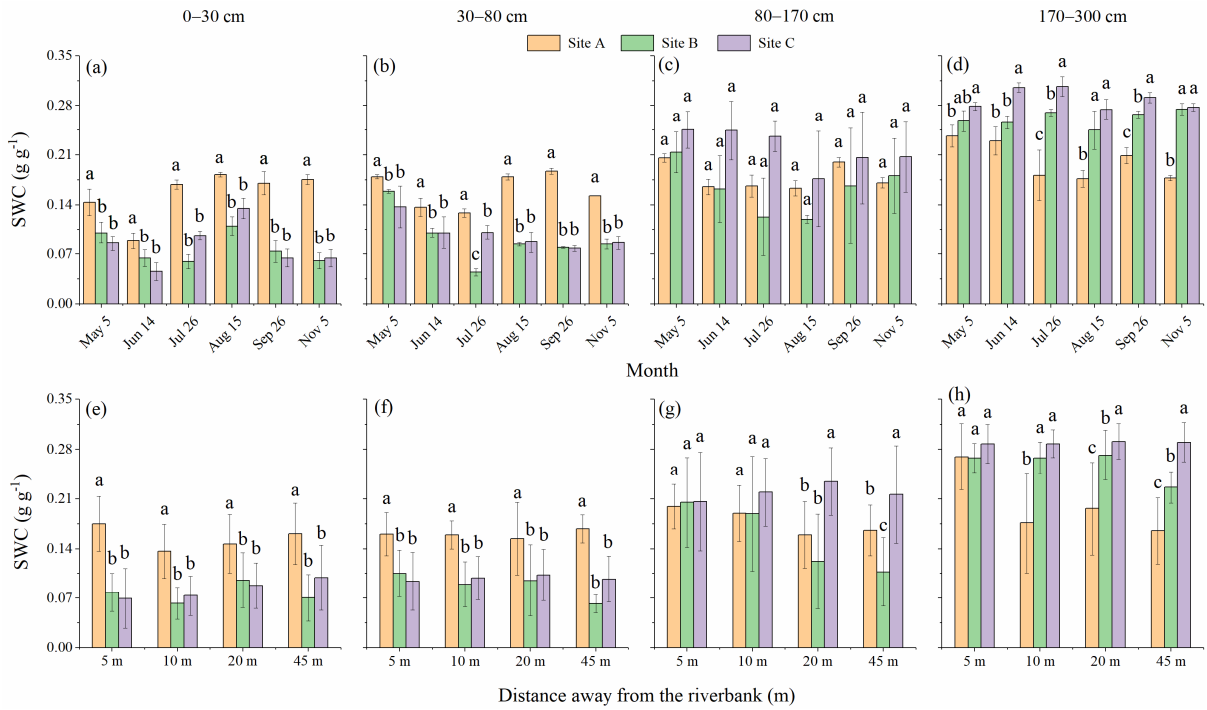

Fig. 3. Comparison of soil water content (SWC) in 0–30 cm, 30–80 cm, 80–170 cm and 170–300 cm layers (a–d) on six campaigns on average of four distances from the riverbank, and (e–h) in the four plots at distance of 5 m, 10 m, 20 m, and 45 m away from the riverbank on average of six campaigns during the observation period in 2019 among sites A, B, and C. The letters (a, b and c) represent significant differences of SWC among the three sites ($p < 0.05$).

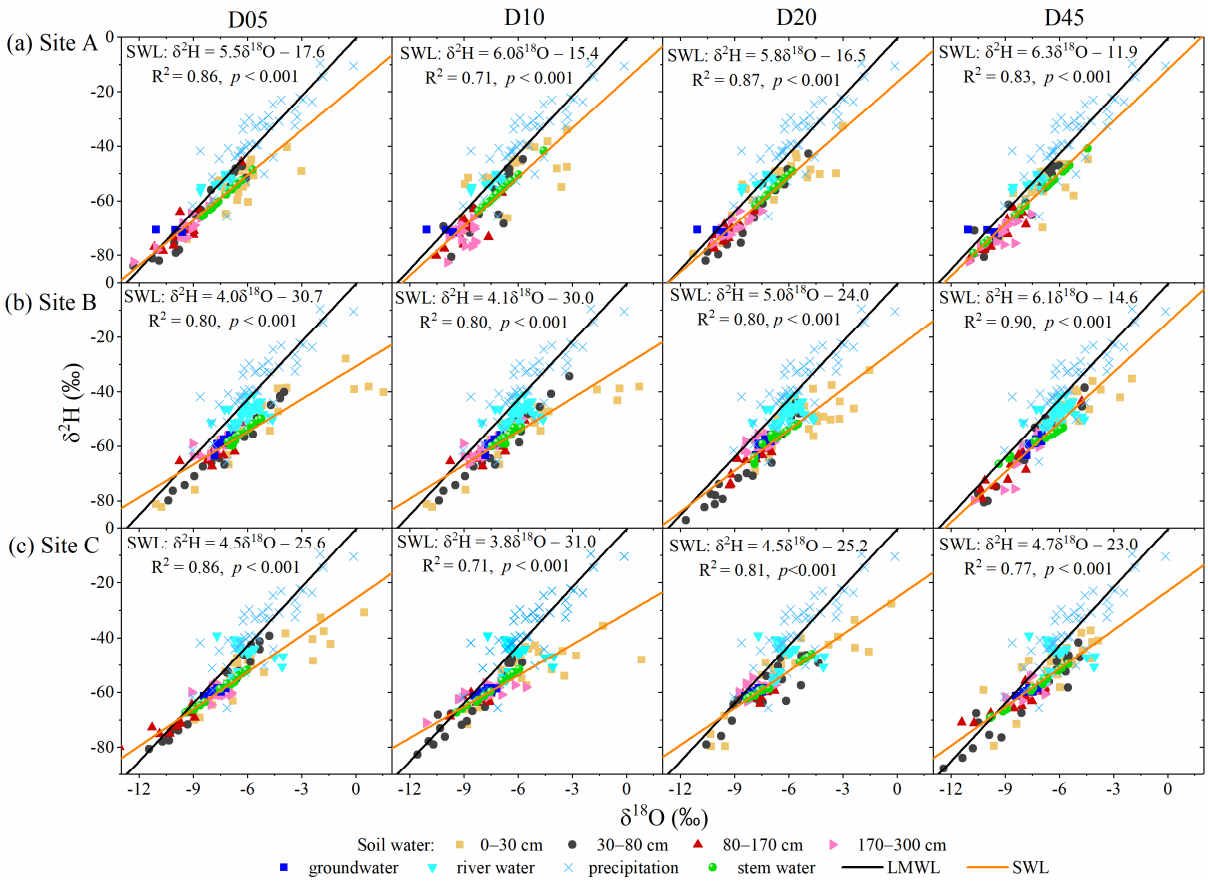

Fig. 4. Dual-isotope (δ^2H and $\delta^{18}O$) biplots of different water bodies in four plots (D05, D10, D20, and D45) during the observation period in 2019 at sites (a) A, (b) B, and (c) C. The soil water line (SWL) was fitted by δ^2H and $\delta^{18}O$ of soil water at different depths. The Local Meteoric Water Line (LMWL) fitted by the isotopic compositions of precipitation in 2019 in the study area was established as $\delta^2H = 5.5\delta^{18}O - 7.9$ ($R^2 = 0.81$, $p < 0.05$). Error bars are standard deviations. D05, D10, D20, and D45 are the plots at distance of 5 m, 10 m, 20 m, and 45 m away from the riverbank, respectively.

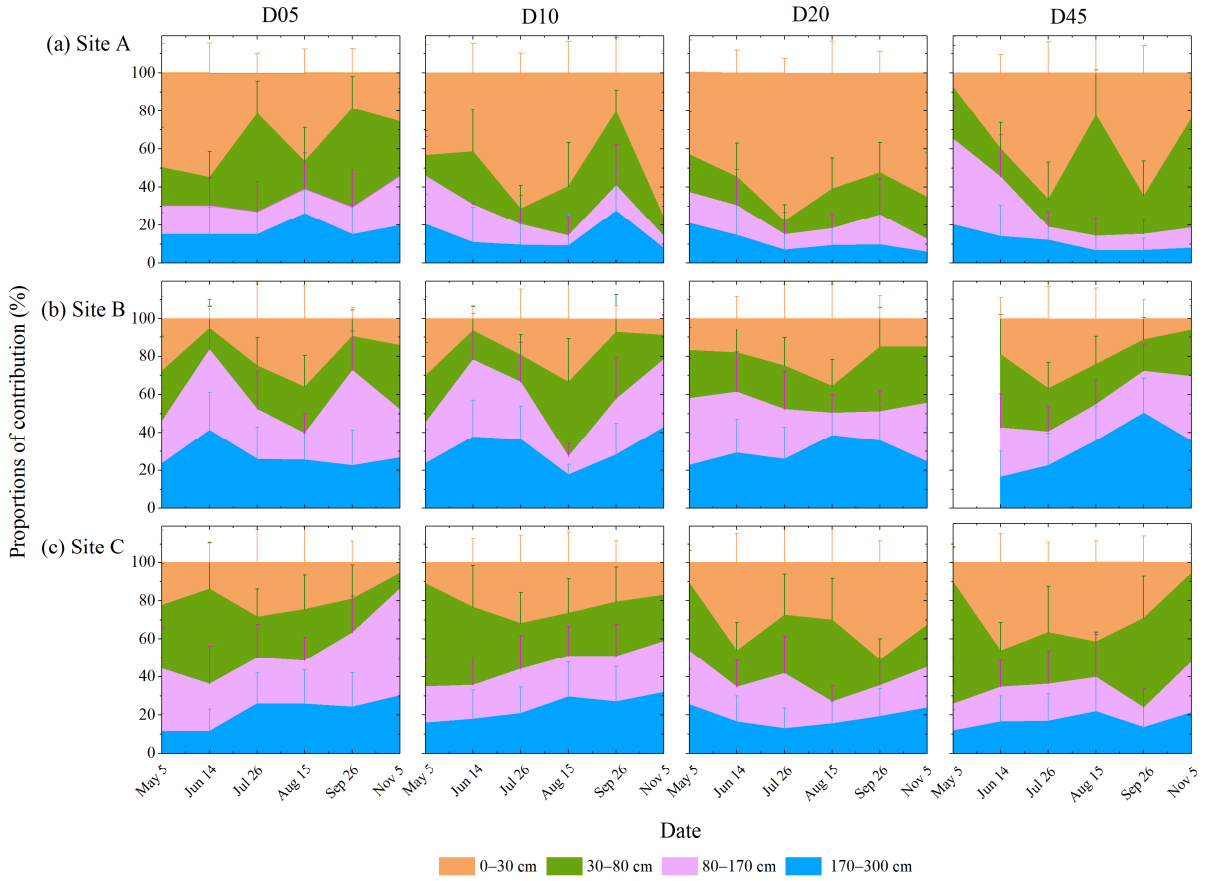

Fig. 5. Seasonal variations in the water uptake patterns of riparian *S. babylonica* in four plots (D05, D10, D20, and D45) at sites (a) A, (b) B, and (c) C. D05, D10, D20, and D45 are the plots at distance of 5 m, 10 m, 20 m, and 45 m away from the riverbank, respectively. The isotopic compositions of soil water in 170–300 cm layer also represent those of groundwater at sites B and C.

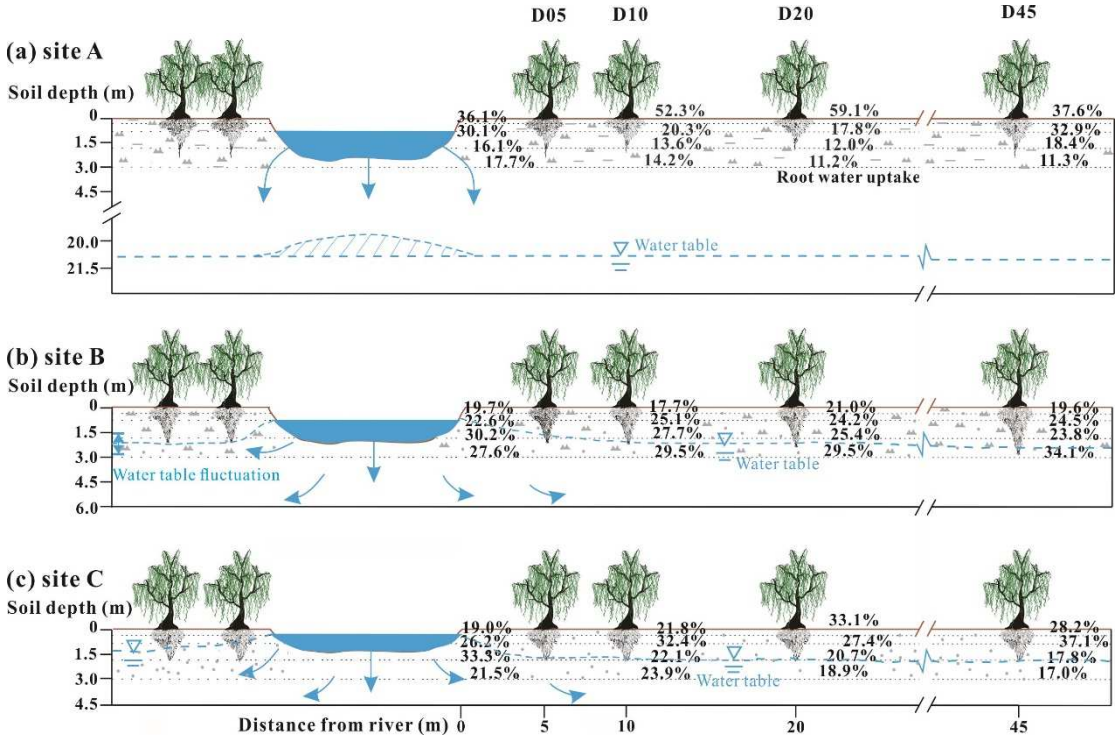

Fig. 6. Schematic diagram for the average root water uptake patterns of riparian *S. babylonica* for all six campaigns during the observation period in 2019 in four plots (D05, D10, D20, and D45) at sites (a) A, (b) B, and (c) C. D05, D10, D20, and D45 are the plots at distance of 5 m, 10 m, 20 m, and 45 m away from the riverbank, respectively.

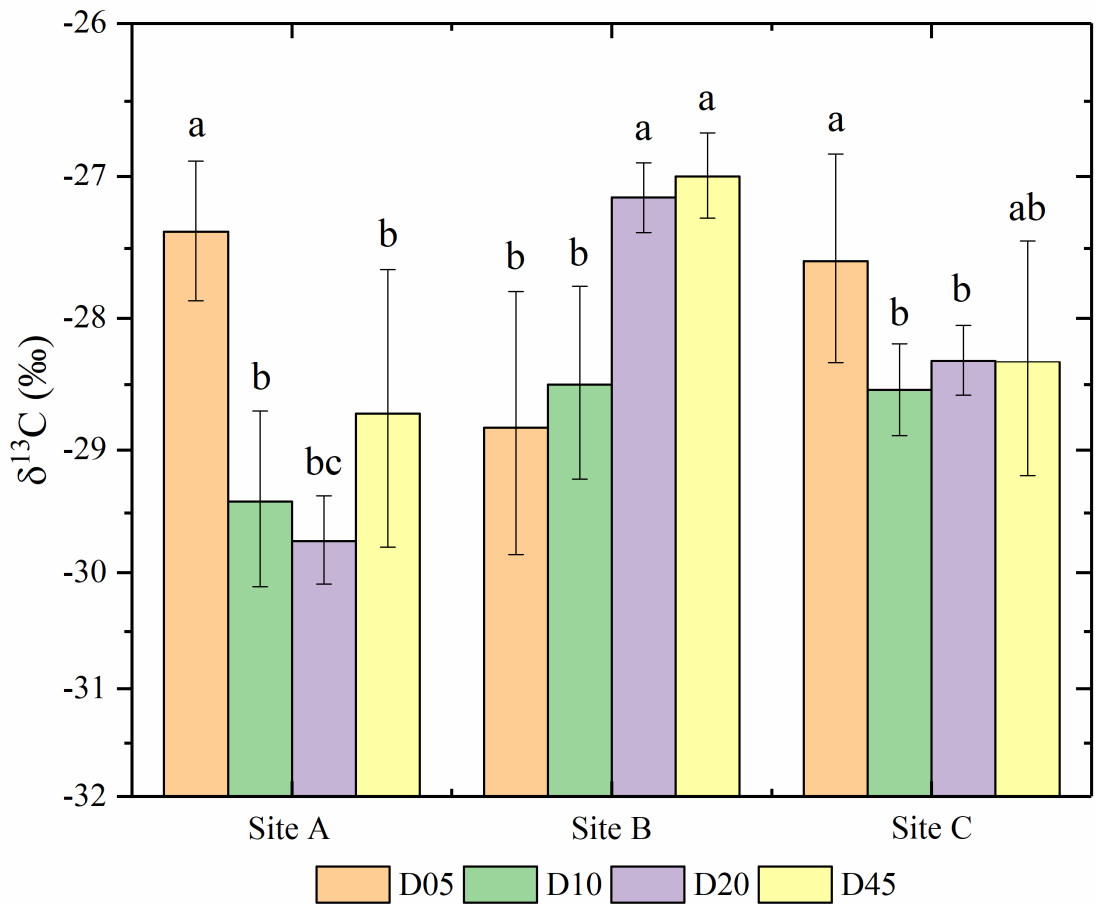

Fig. 7. The average leaf $\delta^{13}C$ of riparian *S. babylonica* for all six campaigns during the observation period in 2019 in four plots (D05, D10, D20, and D45) at sites A, B, and C. D05, D10, D20, and D45 are the plots at distance of 5 m, 10 m, 20 m, and 45 m away from the riverbank, respectively. The letters (a, b and c) represent significant differences in leaf $\delta^{13}C$ of riparian *S. babylonica* among the four plots (D05, D10, D20, and D45) ($p < 0.05$).

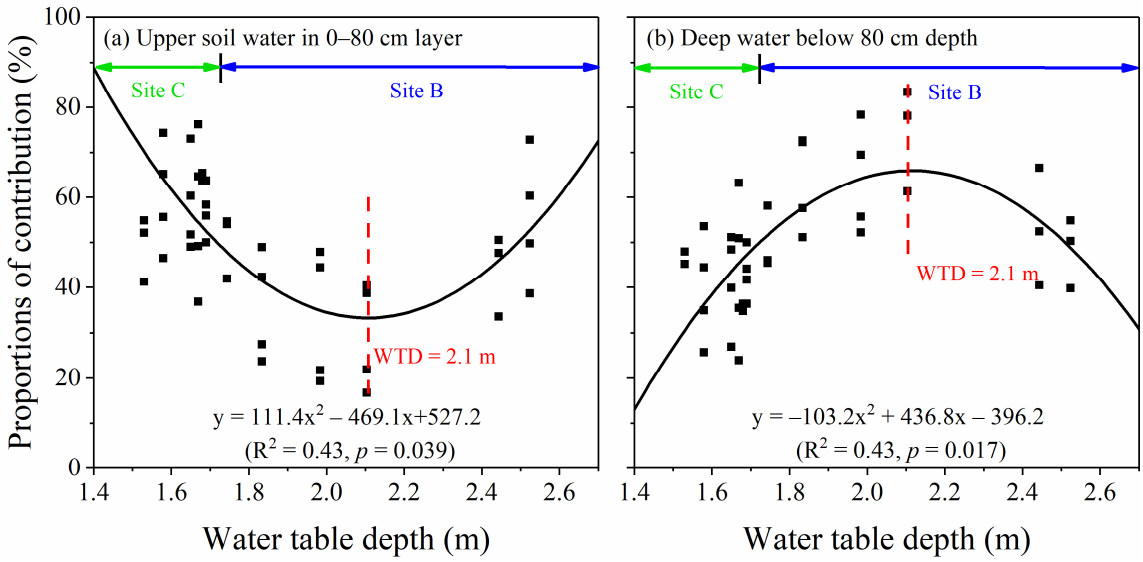

Fig. 8. Relationships between water table depth (WTD) and proportional contributions of (a) upper soil water in 0–80 cm layer and (b) deep water below 80 cm depth for riparian *S. babylonica* under shallow WTD conditions at sites B and C.

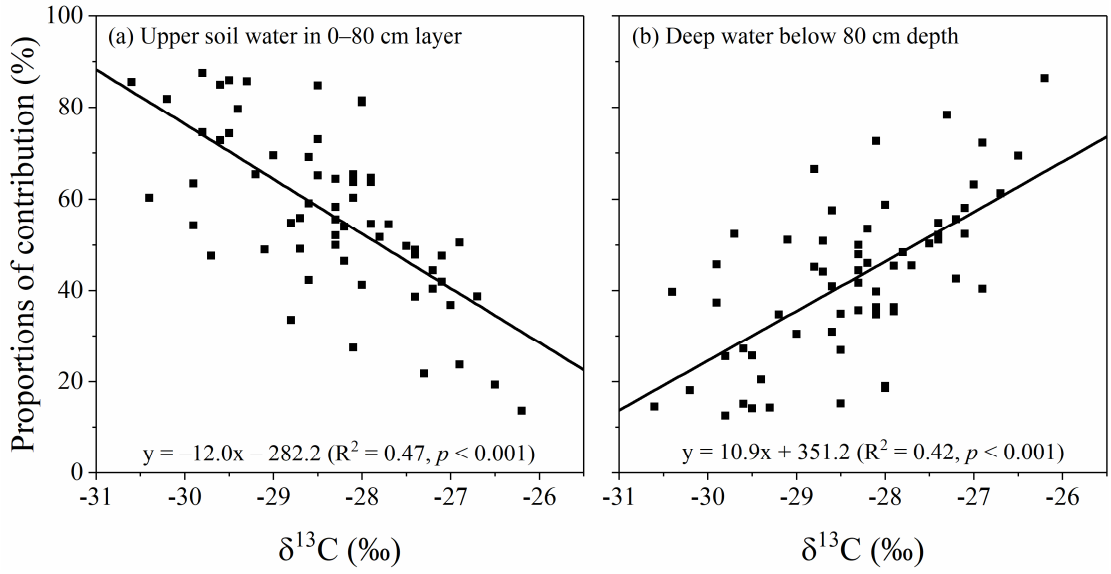

Fig. 9. Relationships between leaf $\delta^{13}C$ and proportional contributions of (a) upper soil water in 0–80 cm layer and (b) deep water below 80 cm depth for riparian *S. babylonica* at the three sites.